Dam-break on an idealised hill side: Preliminary results of a physical model

Dam-break on an idealised hill side: Preliminary results of a physical model

Silvia Cordero[1,*], *Andrea* Cagninei[1,**], and *Davide* Poggi[1,***]

[1]Department of Environment, Land and Infrastructure Engineering (DIATI), Politecnico di Torino, Corso Duca degli Abruzzi 24, 10129 Torino, Italy

Abstract. The aim of this work is to study the propagation of dam-break waves along a hillslope by mean of a physical model (basically i.e. a 3 x 4 m^2 plane set downstream of a reservoir) build up in the Hydraulic Laboratory of the Politecnico di Torino. We want to recreate the water surface, to assess the shape of the flooded area and the arrival time of the wave front. The measurement facility is a high resolution CMOS camera. We measure the water height by linking the intensity of the pixels in the acquired images to the real water depth. Preliminary quantitative results are given for the 0°downstream-slope scenario and qualitative results are presented for the case of downstream inclined plane.

1 Introduction

Floods due to the breaching of earthen dams are a potential hazard to downstream areas. The failure of a small dam can affect a limited area and has less devastating consequences compared to the failure of a large one. Nevertheless the presence of many small dams in the same territory is not a negligible risk for the surrounding communities. A lack in emergency plans may result in considerable damage to people life and properties. This requires analysis of potential impacts which imply the ability to predict the potential flooded area and the wave magnitude. The key factor is the estimate of flow depths and flow velocity.

The majority of these small dams (i.e., according to the Italian law, volume less than 1Mm^3 and height less than 15m) are usually used for agricultural purposes or for artificial snow production. They have no natural inflow and no valley downstream so the propagation of the wave due to a dam-break can not be studied as a one-dimensional (1D) or a two-dimensional (2D) depth averaged flow. Diffusion along the direction perpendicular to the breach axis play a key role in the assessment of the potential flooded area. The downstream slope and roughness plus the collapse dynamic are the main factors to be considered assessing the wave front width.

In the last 10 years numerical models based on different algorithms, Lagrangian methods like SPH (Smoothed Particle Hydrodynamics) [1] and LBH (Lagrangian Block Hydrodynamics) [2], Navier-Stokes equation solvers like volume-of-fluid method [3], large eddy simulations [4] and others (e.g. [5], [6], etc.) have been used by many authors to study the three-dimensional (3D) propagation of a shock wave (i.e. dam-break flows).

*e-mail: silvia.cordero@polito.it
**e-mail: andrea.cagninei@polito.it
***e-mail: davide.poggi@polito.it

Dam-break experiments has mainly concern measurement of the spatial and temporal evolution of the water surface in flumes (2D) with various geometries (e.g. [7], [8], [9], [10]). To the knowledge of the authors, researchers who deal with the 3D case usually record punctual measurements or local measuremente by mean of level sensors, ultrasonic velocity profilers, wave heigh meters and pressure gauges (e.g. [11], [12], [13], [14]). However, recently, some authors demonstrated that measurements of various flow parameters, such as water depth and velocity field, can be acquired in an extensive way (i.e.,spatially distributed) by using image-analysis techniques. Cochard and Ancey [15] used a viscoplatic fluid and a hightspeed camera to analyze the deformation of a fringe pattern projected on the free surface resulting from a dam break on an inclined plane. Aureli et al.[16] obtained the water depth field by processing images of the free surface captured by a digital camera looking at a flat back-lighted device downstream of a sluice. Furthermore Elkholy et al. [17] measured the 3D velocity field by mean of 2 hight definition video cameras and a stereoscopic technique.

The objective of this study is to measure the development of a 3D dam-break flow (i.e. water depth and wave front velocity) on a laboratory physical model. The final goal of the study is to collect high-resolution spatial distributed experimental data that will be used to validate a synthetic methodology to estimate dam-break flooding intensity. The technique here presented is an image-analysis procedure based on light absorption.

The experimental set-up, the light calibration and preliminary results are shown.

2 Experimental set-up

The experiments are conducted in the Hydraulic Laboratory of the Politecnico di Torino. The set-up is sketched in Figure 1. It consists of a 3 m wide and 4 m long wood plane set downstream of a reservoir. The surface of the plane is formed by 8 panels 3 m x 0.5 m wide and 25 mm thick. It is made continuous by sealant and smooth by mean of varnish. A net of 7 wood beams (4 along the 4 m long direction and the other 3 perpendicular to the previous ones) is set under the plane to avoid relative deformations between the panels.

Two portals are fixed on the 2 most external beams, along the longest side of the facility. They are 3 m height and made to support both the camera and the computer case. The first one (the camera) is located on the central line of the plane and the second (computer case) is on the hydraulic right as shown in Figure 1. That allows to acquire all the surface in 2

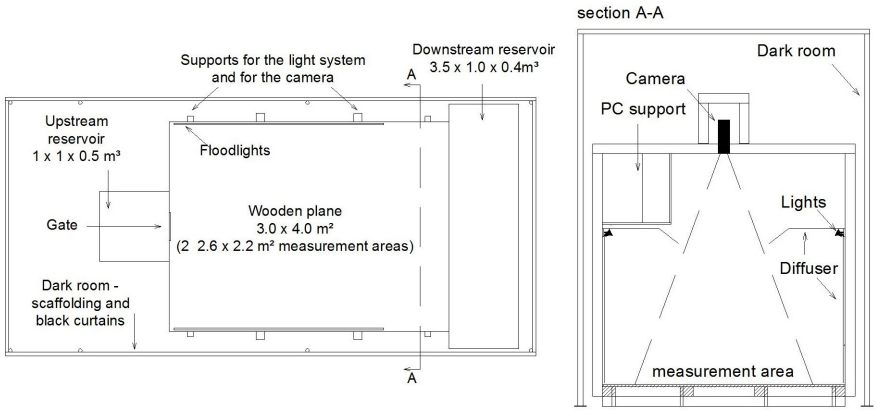

Figure 1: Sketch of the facility - top view and section AA.

different iteration or simultaneously using 2 cameras, one for the upstream portion and one for the downstream. All these components (the plane, the under-structure and the portals) are integral with each other and with the reservoir, so the axis of the camera is always orthogonal to the measurement surface also if the plane is inclined. The facility can be set at different slopes with angle, on the horizontal reference, from 0°to 12°.

Based on previous statistical analysis of the small embankments in Piedmont Region [18], two different kind of reservoirs are adopted: a wedge reservoir 1 m x 1 m x 0.2 m high at the gate and a prismatic reservoirs 1 m x 1 m x 0.4 m. The wedge reservoir can be used only when the plane is inclined as his shape is given by the slope of the downstream "hillside". It can be attached to the wooden beam frame under the measurement surface by mean of 2 beams 2 m long. In the prismatic one, the bottom slope is always 0°regardless of the downstream slope. The reservoir is attached to the downstream plane by mean of 2 jigs which can be opened at different angle to match with the plane slope. In the case of 0°downstream slope this angle is 180°. Another tank is set downstream of the plane to collect the water. After each experiment the collected water is stocked in 4 plastic drums through a pumping system.

For the breach, the shape and size of a completely developed breach in an earthen embankment in accordance with Froehlich's model [19] are adopted. In this case (i.e. due to the reservoirs geometry) the breach is triangular, the vertex angle (bottom of the gate) is 90°. For practical reasons the breach is assumed to cover all the dam height. The maximum width is at the dam crest and is 2 time the the breach height.

The breach is closed by a wooden gate. A soft rubber band is placed along its edges and 2 clamps fastened on the gate top help to ensure watertightness during the fill-up phase.

According to Lauber and Hager [20], the gate opening can be considered instantaneous if it occurs in a lag of time that is less then the time needed for a particle of water that lies on the water surfaces to reach the bottom of the reservoir into free fall i.e. $t = \sqrt{\frac{2h}{g}}$, where h is the water level at rest and g is the gravity acceleration. To satisfy this condition a pulley system is used. The top of the gate is attached to a wire rope, at the other side of the rope a 10 kg weight is set at 3 m height. When unfasten, the weight fall into a sand box, which act as a dumper, and suddenly lifts the gate that slides into 2 tracks over the reservoir wall. The opening time is estimated by recording the opening with a camera an analysing the frames sequence. It results to be 0.2 s. This is enough to work with an initial water depth inside the upstream reservoir of 20 cm.

2.1 Illumination

To obtain the necessary illumination a "light box" is made around the plane. Strictly speaking, in photography, a light-box is a box with one open end, made with diffusing material and illuminated form outside which allows to photograph an object without shadows.

Here the measurement area is surrounded by white darkening curtains leaving free only the breach opening, a space high 0.10 m along the downstream side of the facility to allow the water outlet and a 0.9*4 m^2 space on the ceil to leave free the camera field angle (see Figure 1). The plane is white painted to maximize the light reflection.

The light sources are 20 60 W (8400 lm)led floodlights aligned in 2 rows on the 2 sides of the plane 2 m over it. To obtain the more uniform as possible light over the plane, they are pointed on the 2 ceil diffusers with an angle of 15°on the horizontal line. This allows to avoid direct lighting of the measurement area and punctual reflection over the water surface during the measurements. Different angle were tried. The optimal configuration is chosen with the support of a free lighting design software. The photometric diagram given by the producer is validated by measuring the luminous intensity on the 2 principal planes (0°and 90°) by mean of a spectrometer (Spectromaster C-700).

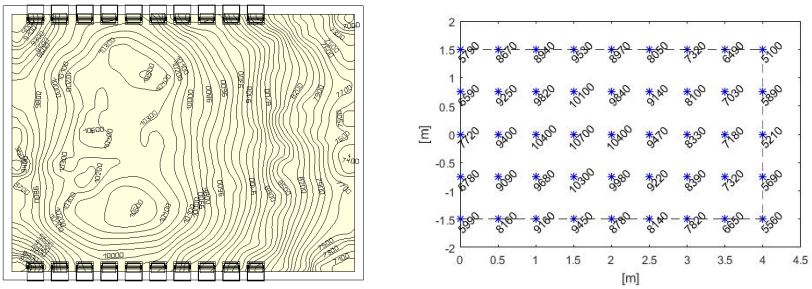

(a) **(b)**

Figure 2: The isolux lines obtained by the free lighting design software (a) and the intensity distribution according to the measurement taken in 45 points on the facility (b).

In the same way, the results of the software simulation are compared to the measure acquired on the plane by the spectrometer. In Figure 2 panel (a) shows the isolux lines obtained by the digital model. The breach is on the left. The maximum intensity (10500 lux) is reached in the middle of the plane about 1.5 m downstream of the reservoir. In panel (b) the distribution of the intensity according to the measurement taken in 45 points on the facility is shown. The maximum value measured is 10700 lux. The value in the 2 downstream corners, which are the darkest zones, are the main difference between the 2 images. The maximum gap is 1600 lux. That is due to the difficulties in the quantification of the refraction index of the diffusers which is apparently a bit overestimated. After the calibration of this coefficient, the digital model is used to study different floodlights locations. In this work measurement of water depth are taken only on the upstream measurement area, for this reason all the floodlights are set side by side starting from the breach section leaving free the last 1 m downstream. The choice of darkening cloth for the light spreaders is due to the necessity to keep the dispersion of light outside the measurement area the less as possible.

The whole set up is set inside a darkroom to prevent the influence of the day light and to have standardised environmental conditions. The darkroom is realised inside of the laboratory by mean of a scaffolding and darkening black cloth. The scaffolding (7 m long, 3.6 m wide and 4.6 m high) has a dual utility: 1) it supports the black cloths that form the walls and the ceil of the darkroom and 2) it support the facility when the plane is inclined. An air-conditioning is used to keep better work conditions for the camera.

3 Measurement system

The experiments are conduced as follows:

- the upstream reservoirs is fill with coloured water previously prepared as described in the following paragraphs;
- the illumination system is turned on, the acquisition parameters of the camera are set and the acquisition start;
- the gate is suddenly lift by the pulley system and the dam-break wave flood the downstream plane;
- the water is collected in the downstream reservoir.

The measurement area covered by a camera set on the first portal (the upstream one), as described in section 2, is 2.2 m wide (along the direction perpendicular to the breach axis)

centred on the breach axis and 2.6 m long starting from the breach section.In order to recreate the water surface, to assess the shape of the flooded area and the arrival time of the wave front, a hight-speed camera is used. After a calibration phase, the intensity of the pixels in the acquired images are linked to the real water depth.

The camera is Andor Zyla 5.5, the sensor resolution is 2560x2160 pixel and the maximum frame rate is 100 fps. The sCMOS monochrome sensor in Zyla is designed with a 5 transistor pixel architecture and allow the *Global Exposure Mode* (Global Shutter) which can be thought as the *Snapshot Exposure Mode* available with a CCD sensor meaning that it enable to capture a single instant of a fast moving event. Using the *Global Shutter Mode* all the pixels in the sensor array are exposed simultaneously: before the exposure begins, all pixels in the array will be held in a "keep clean state", at the start of the exposure, each pixel simultaneously begins to collect charge until the end of the duration of the exposure time. At the end of exposure, each pixel transfers charge simultaneously to its readout node; then an additional digitized readout is required to eliminate reset noise from the global shutter image.

The camera allow to choose between *Global* and *Rolling Shutter Mode*, the last one is the most common acquisition mode and essentially means that adjacent rows of the array are exposed at slightly different times. At the maximum readout rate this means that the row at the top or bottom of each sensor half would have started and ended its exposure 10 ms after the rows at the center of the sensor. The advantages of the *Rolling Shutter Mode* are that the lowest read noise and the maximum frame rate are achievable. In *Global Shutter Mode* the maximum frame rates are halved due to the additional digitized readout process.

For this study the use of *Global Shutter Mode* is mandatory otherwise,except for the case with no downstream slope, the spatial distortions due to the *Rolling Shutter Mode* will compromise the results.

The lens are Sigma 18-35. At the lowest focal length they satisfy the need of minimize the distortion of the images and the need of maximize the focused area. Nevertheless these lens allow a mechanical opening of the diaphragm.

A scarlet dye (cochineal) is uniformly mixed to the water acting as a light absorber. Different concentration were tried to maximize the color intensity and to avoid the sedimentation of the dye powder. A concentration of 0.02 g/l is adopted.

In Figure 3 the different grey intensity across the image can be associated to different water heights: at breach (on the right side) the grey is darker than at the wave front. That is due to the light absorption by the water which increase with the depth and is intensify by the presence of the dye. Looking at the single ray of light it penetrate the water surface and is reflected by the surface of the plane. This reflected ray is attenuated by the presence of the water. The effect of the refraction of the ray by the water surface and the different penetration length of oblique rays in the water body are bypassed by the calibration procedure. The effect of the local slope of the surface during the wave propagation on the path of the light is here neglected.

3.1 Calibration

The calibration procedure is divided in 2 phases. The first one is necessary to convert the distance on the plane from pixels to cm and the second one aims to relate the grey intensity to a water depth. During the first phase a grid with a double level squared mesh (squares with edges of 3 cm and 1 cm respectively with line thickness 2 mm and 1 mm) printed on 6 rigid plastic panels is laid on the plane and a picture is taken with the camera. For each vertex the coordinates both in pixels and in meters are known and, after an analysis procedure of the image, each pixel can be linked to a position in the space. This phase is essential to correct the deformation due to the lens.

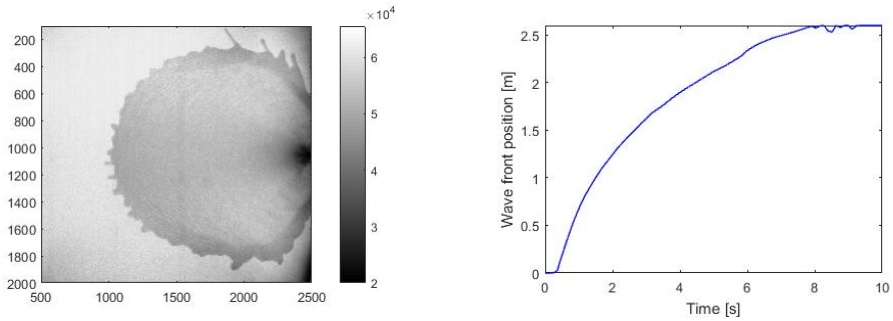

(a) **(b)**

Figure 3: On the left side an image acquired by the camera during the experiment (downstream slope 0°). On the right: time of arrival of the water front at different section downstream the plane.

Table 1: Experimental configuration: summary of the main characteristics.

Configuration	Plane slope	Reservoir shape	Initial water depth at dam	Water volume
A	0°	prismatic	20 cm	200 l
B	12°	wedge	20 cm	105 l
B	12°	wedge	15 cm	59 l
B	12°	wedge	10 cm	25 l

In the second phase 4 20 cm heigh borders are fixed to the edges of the plane and it is filled with coloured water in steps of few mm for depth less than 2 cm and then in steps of 1 cm until the depth of 10 cm is reached. At each steps, when water is at rest, a picture is taken and water depth is measured in 12 target points (4 along the breach axis, 4 on the right border of the measurement area and 4 on its left border) using level gauges. The result is the derivation of local transfer functions which allow inferring water depth information from the grey intensity value of the images acquired during the experiment.

From the results of a preliminary calibration test, where level gauges were set along the plane border, some levelling errors in the set-up are corrected. Unfortunately it is also find out that the plane has a small dip in the center which can not be corrected however it is taken into account in the intensity-depth transfer function.

4 Preliminary results

In this section the preliminary results of 2 experimental configuration name A and B in the following lines are presented. In A the plane is flat (slope 0°) and the reservoir is prismatic. In B the plane slope is the maximum one (12°) and the reservoir bottom has the same slope as downstream. In table 1 there is a summary of the main differences between the 2 and a list of the experiments here presented. In Figure 3, on the right panel, is traced the wave front arrival time along the breach axis obtained for the 0°slope experiment. A section is assumed to be reached by the water when a neighbourhood of 100 pixels (about 10 cm) in the transverse direction is wet. This means that the small cusps visible in the left panel are neglected. Still considering case A, in Figure 4 the shape of the surface at a fixed time is well described by

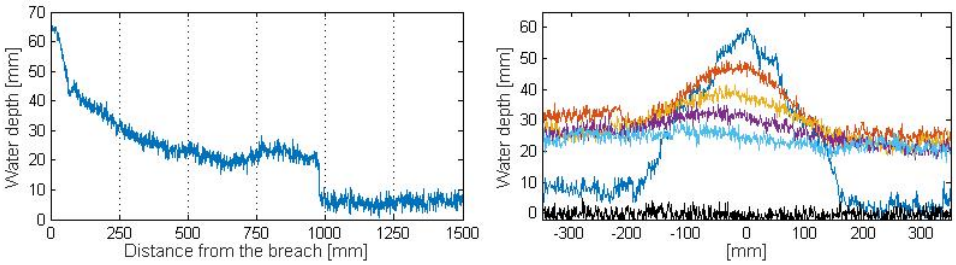

Figure 4: On the left: water depth along the breach axis at time 1 s after the opening (Configuration A). On the right: water depth along sections parallel to the gate, starting from the upper line, respectively 1, 10, 20, 30, 50 and 150 cm downstream the breach at time 1 s after the opening (Configuration A)

a profile taken along the breach axis (on the left) and by some transverse sections set at 1, 10, 20, 30, 50 and 150 cm downstream of the reservoir (on the right). Looking at the right panel, it shows that near the breach the shape of the wave is narrow and higher than in the following sections. More over the central peak decrease rapidly. The wave spread along the transverse direction with a velocity that is comparable with the velocity along the principal flow direction and suddenly the water depth become almost the same along a single section.

The noise that affects the signal acquired by the camera becomes stronger while working with higher slope. For this reason the surface is represented pixel by pixel in Figure 4 whereas in Figure 5 (that refers to configuration B) the results are averaged on a 100 pixels area (about 1 cm^2 an a low-pass filter is applied. In Figure 5 the reduction of the water depth peak along

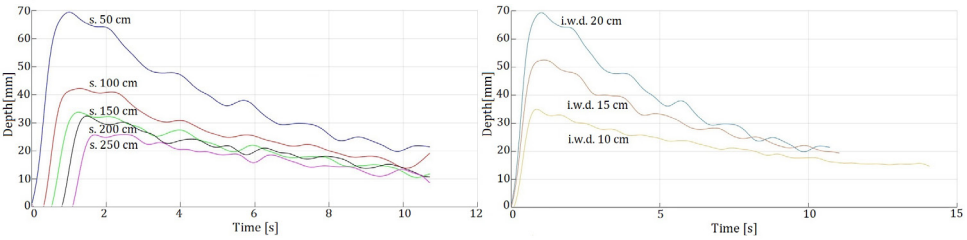

Figure 5: On the left: configuration B with initial water depth at breach 20 cm. Mean value of the water depth in squared clusters of edge 10 pixel set respectively at 50, 100, 150, 200, 250 cm downstream of the breach. A low-pass filter is applied. On the right: comparison between the 3 "configuration B" realisations of the mean value of the water depth in a squared cluster of edge 10 pixel set 50 cm downstream of the breach. A low-pass filter is applied.

the breach axis can be clearly appreciated. Due to the lateral expansion of the wave and to the slope, the depth taken at different distance downstream shortly converge to a stable average value. Changing the initial water depth in the reservoir the main difference can be noticed over than in the water depth peak recorded in the pixel cluster near the breach (Figure 5) especially in the maximum wave front width (Figure 6) and in the velocity along the main flow direction which pass from about 1.4 m/s to 3.1 m/s (this is a preliminary estimation which refer to the time need to the water front along the breach axis to reach the end of the plane).

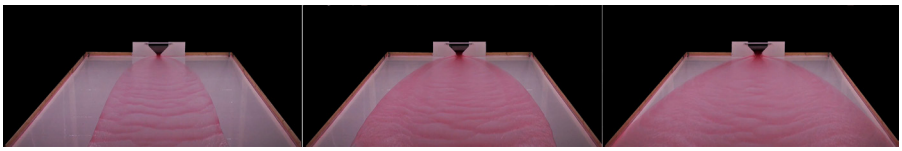

Figure 6: maximum width of the water front in configuration B. From left to right the initial water depth at breach is 10 cm, 15 cm and 20 cm.

5 Further developments

Further developments will be: 1) the use of a new upstream reservoir easier to set at different height which allows to work with a different slope between the plane and the bottom of the tank; 2) treat different shapes of breach; 3) try various roughness on the downstream plane to simulate the different use of soil in the territory downstream the real reservoirs.

References

[1] F. Aureli, S. Dazzi, A. Maranzoni, P. Mignosa, R. Vacondio, Advances in Water Resources **76**, 29 (2015)
[2] L.w. Tan, V.H. Chu, Journal of Hydrodynamics **22**, 650 (2010)
[3] M. Oertel, D.B. Bung, Journal of Hydraulic Research **50**, 89 (2012)
[4] L.A. Larocque, J. Imran, M.H. Chaudhry, Journal of Hydraulic Research **51**, 145 (2013)
[5] W. Yue, C.L. Lin, V.C. Patel, International Journal for Numerical Methods in Fluids **42**, 853 (2003)
[6] C. Biscarini, S. Di Francesco, P. Manciola, Hydrology and Earth System Sciences **14**, 705 (2010)
[7] S.W. Bell, R.C. Elliot, M. Hanif Chaudhry, Journal of Hydraulic Research **30**, 225 (1992)
[8] S. Soares-Frazão, Journal of Hydraulic Research **45**, 19 (2007)
[9] L.A. LaRocque, J. Imran, M.H. Chaudhry, Journal of Hydraulic Engineering **139**, 569 (2013)
[10] H. Ozmen-Cagatay, S. Kocaman, H. Guzel, Journal of Hydro-environment Research **8**, 304 (2014)
[11] L. Fraccarollo, E.F. Toro, Journal of Hydraulic Research **33**, 843 (1995)
[12] S. Soares-Frazão, Y. Zech, Journal of Hydraulic Research **45**, 27 (2007)
[13] S. Soares-Frazão, Y. Zech, Journal of Hydraulic Research **46**, 648 (2008)
[14] M.S. Güney, G. Tayfur, G. Bombar, S. Elci, Journal of Hydraulic Engineering **140** (2014)
[15] S. Cochard, C. Ancey, Experiments in Fluids **44**, 59 (2008)
[16] F. Aureli, A. Maranzoni, P. Mignosa, C. Ziveri, Experiments In Fluids **50**, 665 (2011)
[17] M. Elkholy, L.A. LaRocque, M.H. Chaudhry, J. Imran, **142**, 04016042 (2016)
[18] S. Grimaldi, D. Poggi, *A synthetic method for assessing the risk of dam flooding* (Torino, 2010)
[19] D.C. Froehlich, Journal of Hydraulic Engineering pp. 1708–1721 (2008)
[20] G. Lauber, W.H. Hager, Journal of Hydraulic Research **36**, 291 (1998)